Predicting material parameters for intrinsic point defect diffusion in Silicon Crystal Growth

Michael Griebel[1], Lukas Jager[2] and Axel Voigt[3]

[1] Institut für Angewandte Mathematik, Universität Bonn, Wegelerstr. 6, 53115 Bonn, Germany, griebel@iam.uni-bonn.de

[2] Institut für Angewandte Mathematik, Universität Bonn, Wegelerstr. 6, 53115 Bonn, Germany, jager@iam.uni-bonn.de

[3] Crystal Growth group, research center caesar, Ludwig-Erhard-Allee 2, 53175 Bonn, Germany, voigt@caesar.de

Keywords: Semiconducting Silicon, Intrinsic point defects, Material parameters, Molecular Dynamics, Stillinger-Weber potential, Tersoff potential

Abstract. The incorporation of intrinsic point defects into a growing crystal and their subsequent agglomeration into larger defects are controlled by the solidification and subsequent cooling process. The evolution of intrinsic point defects in Silicon can generally be described by a system of reaction-diffusion equations for the concentration of self-interstitials and vacancies. The main difficulty in quantitative intrinsic point defect prediction with such an approach is the uncertainty of the temperature-dependent material properties. These properties are generally unknown. This is due to the difficulty to measure them experimentally at high temperatures. To circumvent this problem these properties can be computed by an underlying microscopic model by means of molecular dynamics simulations. A potential due to Stillinger and Weber or, alternatively, a many-body potential due to Tersoff is applied for this purpose. The calculated material data for these potentials as well as intrinsic defect concentrations during the Czochralski growth of silicon are presented. A transient process simulation with varying process conditions is performed and the influence on the intrinsic defect concentrations in the crystal is shown.

Introduction

The quality of crystalline silicon highly influences the quality of semiconductor devices fabricated on it. Grown-in defects, such as octahedral voids or networks of large dislocation loops can be detrimental to the functionality of devices [1]. Both type of defects result from the interaction of intrinsic point defects, vacancies and self-interstitials, during growth and subsequent annealing of the crystal. In order to qualitatively describe the formation of microdefects in crystalline silicon a detailed understanding of intrinsic point defects is necessary.

Modeling of defect dynamics in silicon crystals during growth requires the description of physical phenomena on different length and time scales. Continuum balance equations are used to describe the distribution, transport and kinetic interactions of point defects, either vacancies or self-interstitials, throughout the crystal as a function of the local temperature. These equations are written in terms of kinetic expressions for the solid-state reactions between species, transport expressions for Fickian diffusion and thermodiffusion and equilibrium concentrations for the point defects. Each of these expressions contains highly temperature-dependent material properties, which describe atomistic events, such as the diffusion of a self-interstitial through the silicon lattice or the recombination of a vacancy with a self-interstitial to form a perfect crystal.

The temperature distribution throughout the crystal during the growth process can be computed by a macroscopic heat transfer model in the entire crystal growth system, taking into account heat conduction in all components, heat radiation between surfaces, internal radiation as well as convection in the melt [2,3,4]. With such transient heat transfer models the temperature distribution in the crystal can be related to design and operating conditions of the crystal growth system.

The absence of direct experimental measurements of intrinsic point defect properties at high temperatures make it necessary to compute these properties from atomistic simulations based on empirical or semiempirical atomic models. Here, the microscopic quality of the crystal is given by the intrinsic point defect concentration. Thus, in order to directly relate these quantities to crystal growth conditions, macroscopic process simulations in the entire crystal growth furnace as well as atomistic calculations of silicon are necessary, Fig. 1.

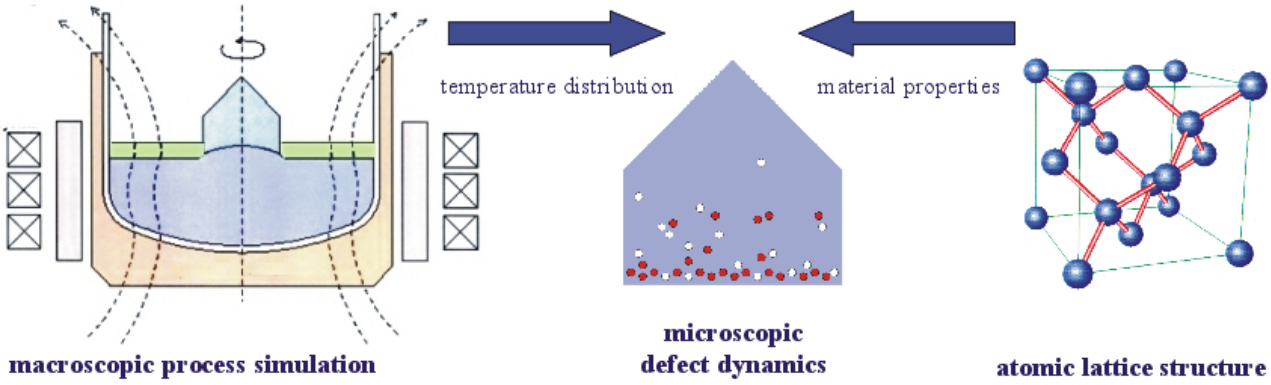

Figure 1. Multiscale model for defect dynamics: macroscopic process simulation in a Czochralski furnace provides the temperature distribution in the crystal, an atomistic model provides the temperature-dependent material parameter for the defect dynamics.

The aim of this paper is to provide this information from large scale molecular dynamic simulations based on the potentials of Stillinger-Weber and Tersoff. The macroscopic process simulation is discussed elsewhere [5], the focus of this paper lies on the microscopic and atomistic models.

Reaction-diffusion equations of point defects

The evolution of intrinsic point defects in Silicon on the macroscopic level can generally be described by a system of reaction-diffusion equations for the concentration of self-interstitials and vacancies, C_i and C_v, respectively, [15].

$$\frac{\partial C_i}{\partial t} - \nabla \bullet \left(D_i \nabla C_i - \frac{Q_i D_i C_i}{k_B T_c^2} \nabla T_c\right) = k_{rec}\left(C_i^{eq} C_v^{eq} - C_i C_v\right) \tag{1}$$

$$\frac{\partial C_v}{\partial t} - \nabla \bullet \left(D_v \nabla C_v - \frac{Q_v D_v C_v}{k_B T_c^2} \nabla T_c\right) = k_{rec}\left(C_i^{eq} C_v^{eq} - C_i C_v\right) \tag{2}$$

Here D_i and D_v denote diffusion coefficients, Q_i and Q_v denote activation enthalpies for thermal diffusion, C_i^{eq} and C_v^{eq} denote equilibrium concentrations, T denotes temperature, k_B is the Boltzmann constant and k_{rec} is the reaction coefficient for recombination. Equation (1) and (2), along with initial and boundary conditions

$$C_i = C_{i,0},\ C_v = C_{v,0} \quad \text{at t = 0 in the crystal} \tag{3}$$

$$C_i = C_i^{eq},\ C_v = C_v^{eq} \quad \text{at the crystal surface} \tag{4}$$

describe the evolution of self-interstitials and vacancies.

The system is solved by a finite element method in a rotational symmetric setting. It is coupled to a transient global heat transfer model in the entire crystal growth system [5].

Atomistic description of material properties

All material properties involved in the reaction-diffusion equations are highly dependent on temperature. These properties can only be measured indirectly in experiments and thus cannot be provided for high temperatures within the needed accuracy for quantitative point defect simulation. Although some calculations using quantum mechanical principles have been made in the recent years, such approaches cannot handle the larger length and time scales, which are required for the statistical averages to compute material parameters like the diffusion of intrinsic point defects. Atomistic simulations, using empirical interatomic potentials, can be used to circumvent this problem. First attempts in this direction were made in [6]. Monte Carlo simulations where used in the isothermal-isobaric (NpT)-ensemble in a periodic supercell of 216 atoms with a single vacancy or self-interstitial. Furthermore a Stillinger-Weber interatomic

potential was employed. The focus of this paper is the use of molecular dynamics in order to compute the diffusion coefficients $D_{i,v}$ using Stillinger-Weber [7] and Tersoff [8,9,10] interatomic potentials.

Description of Potentials

Simple pair potentials like the Lennard-Jones interaction, which is typically used for liquified noble gases, are not sufficient for the simulation of covalent systems. Stillinger and Weber [7] proposed an empirical potential, which consists of a two- and a three-body term for the condensed phases of silicon. The incorporated parameters were chosen to stabilize the diamond structure at low pressure and to give good agreement with experimental data for the melting point and the liquid structure. Tersoff [8,9] derived a different form of potential also including two- and three-body terms. He fitted the parameters to correctly reproduce cohesive energies, the bulk modulus and the bond length in the diamond structure. In [10] the set of parameters was improved to give better results for the elastic properties of silicon. In our simulations we use both potentials for molecular dynamics in the (NVT)-ensemble to compute diffusion coefficients of self-interstitials and vacancies.

Computing the diffusion coefficients

We perform molecular dynamics simulations in a canonical ensemble to compute the diffusion coefficients. Macroscopic values can be measured in this ensemble by averaging the microscopic values with the Boltzmann factor. In this sense the diffusion coefficient is directly related to the spatial motion of the particles. Einstein first derived that the diffusion coefficient D can be written as

$$D = \frac{1}{6}\frac{\partial}{\partial t}\left\langle (\mathbf{x}(t_0) - \mathbf{x}(t))^2 \right\rangle, \tag{5}$$

where $\boldsymbol{x}(t)$ is the position of a particle (interstitial or vacancy) at time t and $\langle\,\rangle$ denotes averaging with the probability function. Since we cannot compute the average without knowing the probability function, we use the alternative formulation

$$D = \lim_{t\to\infty} \frac{1}{6(t-t_0)} (\mathbf{x}(t_0) - \mathbf{x}(t))^2 \qquad \text{and approximate this by} \qquad D \approx \frac{1}{6(t-t_0)} (\mathbf{x}(t_0) - \mathbf{x}(t))^2 . \tag{6}$$

For t large enough this gives a good approximation to the diffusion coefficient. The procedure is now as follows: We start with a perfect crystal in a periodic box and insert one self-interstitial or remove one atom in order to create one point defect. Then we perform a molecular dynamics run of several nanoseconds at a given temperature and track the position of the point defect over time. The coupling to a heat bath is simulated using the Nosé thermostat [14]. The identification of the point defect in the crystal is done by checking the local environment of every particle for defects. In the perfect tetrahedral structure each particle has four nearest neighbors within a distance of about 0.29 nm. Any particle with a variation of more than one in the number of nearest neighbors is defined as interstitial. Due to thermal fluctuations in the crystal this criterion is sometimes also satisfied for particles of the crystal lattice. These situations are handled by a comparison with detected interstitials of past time steps. Fig. 2 (left) shows an example of a trajectory for a self-interstitial. In order to apply equation (6) we have to correct the trajectory with respect to the periodic boundary conditions. The corrected and smoothed trajectory is also shown in Fig. 2 (left). The smoothing removes local fluctuations and is done by a low-pass filter. From this data the function $r(t) = (\boldsymbol{x}(t_0) - \boldsymbol{x}(t))^2$ is computed, Fig. 2 (right). Linear regression results in an approximation of the diffusion coefficient at this temperature according to equation (6). As one can see in Fig. 2 (right), large fluctuations of $r(t)$ imply the necessity for molecular dynamic runs with long time intervals in order to minimize the error. The choice of the simulation parameters is therefore a compromise between large system sizes to reduce finite size effects and an acceptable computation time for the necessary physical simulation time. Most of the calculations in the literature were performed within a periodic supercell containing 216 atoms [6,11,12] and with simulation times up to 200 ps [12]. We decided to increase the system size to 1000 particles in a periodic box of length 2.67 nm. This leads to a density of 2.44 g/cm^3, which is in agreement with the specifications given in [7]. Table 1 shows the temperatures, time lengths and computed diffusion coefficients for a self-interstitial of our simulations. The simulations at temperatures over the experimental melting point were performed in an overheated crystal.

Experimental data suggests that the temperature dependence on the diffusion coefficient exhibits an Arrhenius behavior $D_i = D_i^0 \exp(-E_m / k_B T)$. Hence we fit the logarithm of the measured data by means of the method of least squares to a straight line.

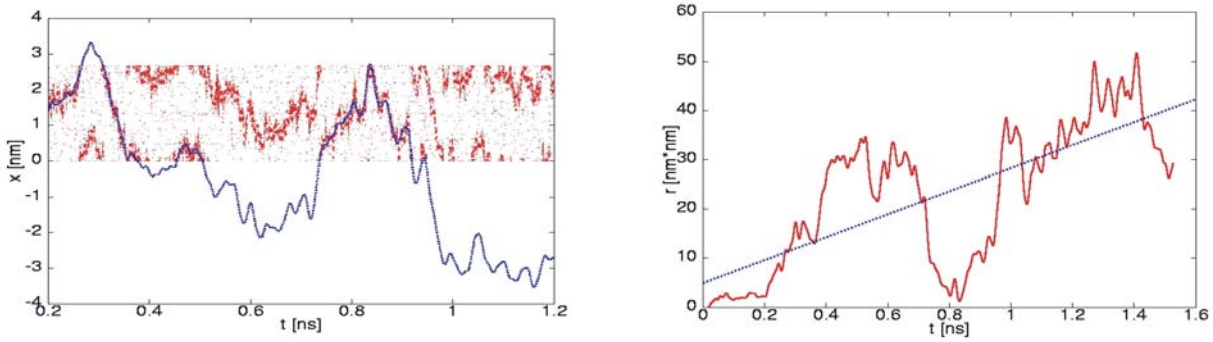

Figure 2. Left: The x-coordinate of the trajectory (points) of a self-interstitial and the x-coordinate of the periodically corrected trajectory (dashed line). Right: Function *r(t)* (solid line) and resulting linear fit (dashed line).

T [K]	$D_i[10^{-5}\mathrm{cm}^2/\mathrm{s}]$(SW)	$D_i[10^{-5}\mathrm{cm}^2/\mathrm{s}]$(TF)
1510.7	4.278 (0.6ns)	0.046 (0.9ns)
1573.6	3.889 (0.8ns)	-
1636.8	1.525 (3.8ns)	0.610 (1.5ns)
1762.4	6.006 (2.9ns)	1.038 (1.2ns)
1888.3	35.771 (1.6ns)	0.4933 (1.6ns)

Table 1. Temperatures, diffusion coefficients and time lengths for simulations with one self-interstitial using either Stillinger-Weber (SW) or Tersoff (TF) potential**.**

Fig. 3 (left) shows the data and fitted lines for both potentials. The resulting migration energies E_m are 1.35 eV and 1.58 eV, and the diffusivity prefactors are calculated as 0.72 cm^2/s and 0.19 cm^2/s for the Stillinger-Weber and Tersoff potential, respectively. As shown in Fig. 3 (right), the results are in good agreement with the calculations published in the literature [6,11,12]. Due to the small number of data points, more simulations have to be performed to stabilize the results. The uncertainty of each data point itself can only be minimized by increasing the simulations time.

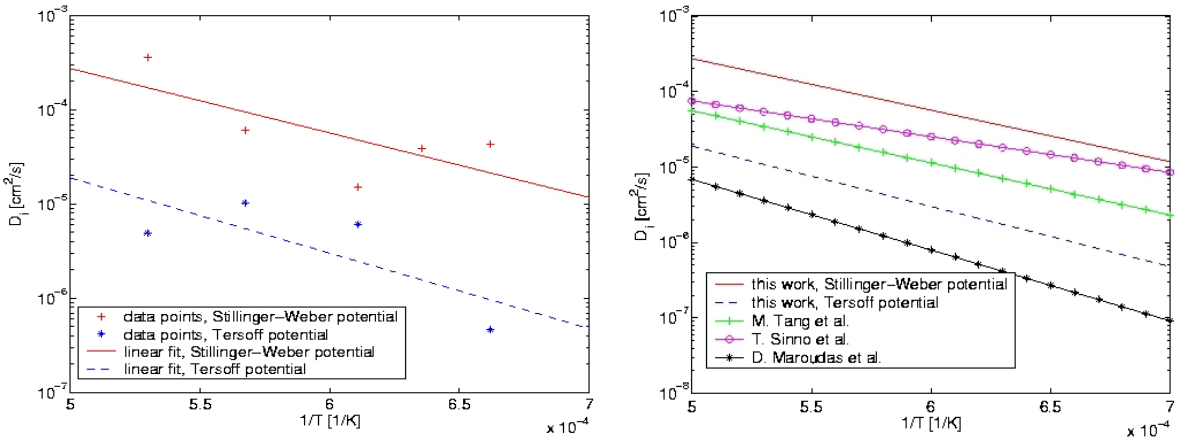

Figure 3. Left: Diffusion coefficients for interstitials computed with Stillinger-Weber and Tersoff potential and linear fits. Right: Functions $D_i(T)$, comparison of the results of this work with the results of M. Tang [12], T. Sinno [11] and D. Maroudas [6].

Results

We now are able to provide the temperature dependent diffusion coefficients in the reaction-diffusion equation (1)-(2). This data can now be used in order to link the macroscopic process simulation [5], providing the temperature distribution in the crystal, and the point-defect dynamics. To this end, we consider the Czochralski growth process in an industrial furnace. It is used by Wacker Siltronic AG, Burghausen to grow crystals with 200 mm diameter. We simulate the transient global heat transfer in the whole furnace together with the concentration of interstitials and vacancy densities. For the pulling velocities we use the data of the real production process of Wacker Siltronic AG which are given in Fig. 4 (left). The simulation starts with an initial quasi steady state computation for an initial crystal. Then the crystal is pulled according to the velocities of Fig. 4 (left) and the temperature distribution, the free boundary and point defect concentrations are computed step by step over time.

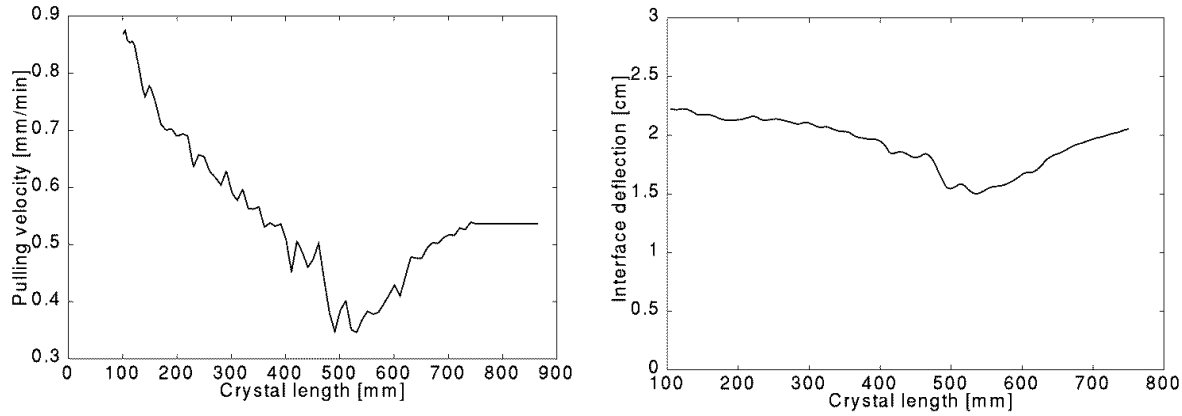

Figure 4. Left**:** Pulling velocity of growing crystal in mm/min over crystal length in mm (experimental data). Right: Simulated free boundary deflection in cm over crystal length in mm. The deflection is measured in the crystal center.

The results show an influence of the varying pull rate on the interface shape, see Fig. 4 (right). We see that the deflection of the interface is directly related to the pulling velocity. The temperature profiles for various time steps (crystal length) in the crystal as well as scaled differences of point defect distributions are shown in Fig. 5 and Fig. 6, respectively. The upper part of the crystal continuously cools down during the growth process. The axial temperature gradient is larger close to the phase boundary and decreases with increasing crystal length. Due to the sensitivity of the temperature gradients at the interface the variations of its shape strongly affect the temperature and point defect distribution and should therefore not be neglected as is usually done in other quasi-static simulations.

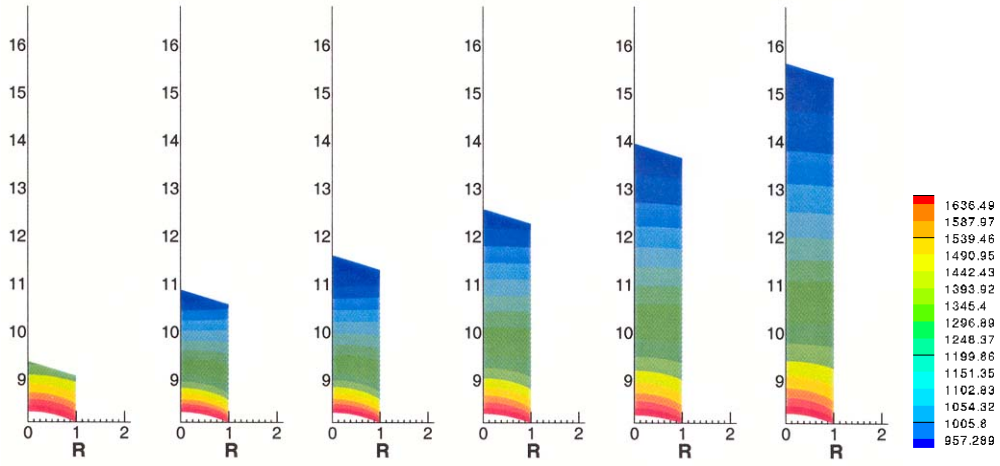

Figure 5. Temperature in crystal at various time steps.

The scaled differences of interstitial and vacancy concentrations show that vacancies dominate at the beginning of the growth process as a result of the high pull rate. This leads to a vacancy-rich upper part of the crystal. When we decrease the pull rate (crystal length < 500) the concentration of self-interstitials increases and starts to dominate. When

we then increase the pull rate (crystal length > 500) the concentration of vacancies increases again and the interstitial reservoir moves upwards with the pull rate.

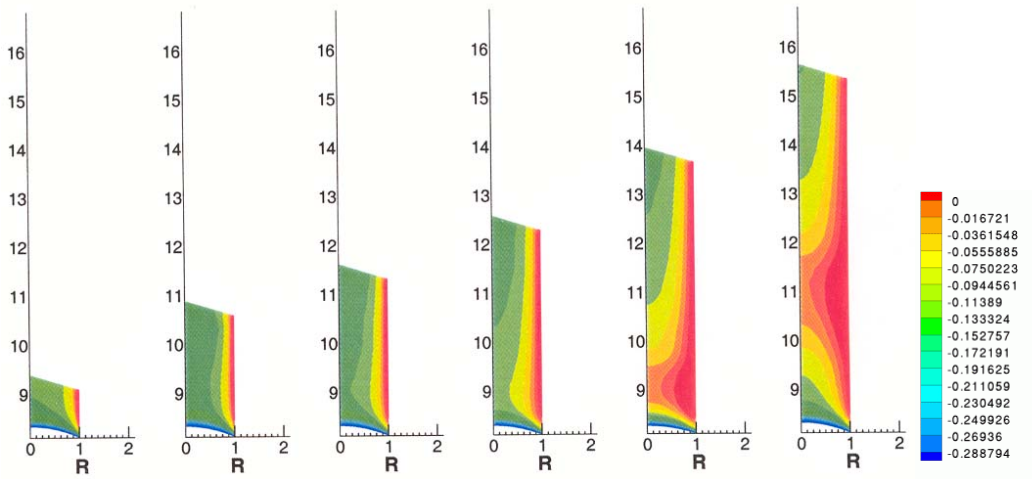

Figure 6. Difference of point defect concentration in crystal at various time steps; red is indicating an excess of self-interstitials, whereas green indicates vacancy dominated regions. A scaled difference of C_i and C_v is shown.

Due to the faster diffusion of interstitials than vacancies the interstitial reservoir spreads into the vacancy-rich regions. This effect cannot be modeled by a quasi-steady assumption. The phenomenological *v/G* law [14], which relates the quotient of the pulling velocity *v* and the temperature gradient at the interface *G* to the surviving point defect species in the cooled crystal, is based on a quasi-steady assumption and can therefore not be applied, if strong variations in the pulling velocity occur. The high interstitial concentrations at the crystal boundary result from the specified equilibrium concentrations and are probably overestimated in these results.

Acknowledgments

We would like to thank Wacker Siltronic AG, Burghausen for providing the experimental data. Furthermore, we thank J. Hamaekers and R. Wildenhues, who are involved in the development of our molecular dynamics package and C. Weichmann for his assistance in the Finite Element simulations. This work was partially supported by DFG through SFB 611.

References

[1] J. Park: Solid State Phenomena Vol. 47-48 (1996), p. 327.
[2] F. Dupret, N. van den Bogaert: in Hurle, D. T. J. ed. Handbook of Crystal Growth, 2b, Elsevier, 1994.
[3] H. Zhang, L.L. Zheng, V. Prasad, D.J. Larson, Jr.: J. Heat Transfer Vol. 120 (1998), p. 874.
[4] A. Voigt, K.-H. Hoffmann: Int. Ser. Num. Math. Vol. 139 (2001) p. 259.
[5] A. Voigt, C. Weichmann, J. Nitschkowski, E. Dornberger, R. Hölzl: Crys. Res. Technol. Vol. 38-6 (2003), p. 499.
[6] D. Maroudas, R.A. Brown: Appl. Phys. Lett. Vol 62-2 (1993), p. 172.
[7] F.H. Stillinger, T.A. Weber: Phys. Rev. B Vol. 35 (1985), p. 5262.
[8] J. Tersoff: Phys. Rev. Lett. Vol. 56-6 (1986), p. 632.
[9] J. Tersoff: Phys. Rev. B Vol. 37-12 (1988), p. 6991.
[10] J. Tersoff: Phys. Rev. B Vol. 38-14 (1988), p. 9902.
[11] T. Sinno, R.A. Brown, W. v. Ammon, E. Dornberger: J. Electrochem. Soc. Vol. 145 (1998), p 302.
[12] M. Tang, L. Colombo, J. Zhu, T. D. de la Rubia : Phys. Rev. B Vol. 55-21 (1997), p. 14281.
[13] V. Voronkov: J. Crystal Growth Vol. 59 (1982), p. 625.
[14] S. Nosé, M. L. Klein: J. Mol. Phys. Vol. 50 (1983), p. 1055.
[15] E. Dornberger, W. von Ammon, J. Virbulis, B. Hanna, T. Sinno: J. Crys. Growth. Vol 230 1-2 (2001) p. 291